Probing the Mechanism of Insulin Aggregation with Added Metalloporphyrins

Scott P. Sibley,*[,‡] Katrina Sosinsky,[‡,§] Lisa E. Gulian,[‡,⊥] Esther J. Gibbs,[‡] and Robert F. Pasternack[||]

Department of Chemistry, Goucher College, Baltimore, Maryland 21204, and Department of Chemistry and Biochemistry, Swarthmore College, Swarthmore, Pennsylvania 19081

Received August 20, 2007; Revised Manuscript Received December 21, 2007

ABSTRACT: The mechanism of inhibition of insulin-based amyloid gel formation by metal derivatives of tetrakis(4-sulfonatophenyl)porphyrin has been investigated. Time-course UV/vis measurements in conjunction with atomic force microscopy (AFM) were used to study the correlation between observed kinetics and amyloid structure for various concentration ranges of added metalloporphyrins. Observed structures include fibrils as well as circular, ring-like structures formed as a result of the interaction of insulin with porphyrin. In addition, binding studies demonstrate that the effectiveness of inhibition of the various metalloporphyrins is directly related to the strength of binding to insulin. It is suggested that both the electron distribution in the porphyrin core and the tendency to form porphyrin dimers affect both the structure of amyloid formed and the kinetic profile of the reaction.

The study of amyloid formation is of broad interest, because amyloid protein structures have been linked to a variety of human diseases, including Alzheimer's (*1, 2*) and Parkinson's diseases (*3*).

While different proteins are involved in the various amyloidogenic diseases, the aggregates formed as a result of protein misfolding often have strikingly similar structural characteristics. Long, fibrillar assemblies rich in the β-sheet structure characteristic of the amyloid proteins have been observed for a large number of proteins, under conditions that promote protein destabilization, such as high acidity and temperature or the addition of denaturants (*4–8*). One such protein is insulin.

Insulin has the advantage of providing a relatively convenient system to model amyloid formation. A number of studies have focused on the elucidation of the molecular mechanism of insulin aggregation and the morphologies of the aggregates formed (*9–13*). The kinetic profile of insulin aggregation is characterized by a long lag period followed by a rapid growth phase, and the study of the kinetics of the process has been the subject of a number of investigations (*14–16*). The aggregation of insulin has been shown to be inhibited by a number of molecules (*16*), with implications for drug treatment of amyloidogenic diseases. In previous work, metal derivatives of tetrakis(4-sulfonatophenyl)porphine (TPPS)[1] were shown to inhibit insulin fibril formation *in vitro*, with the effectiveness of the inhibition dependent upon the identity of the metal and the concentration of the porphyrin. Atomic force microscopy (AFM) has been shown to be a highly effective tool for both the study of fibril formation in general (*17*) and for insulin aggregation in particular (*18, 19*). This paper will combine kinetic studies with the results of AFM.

Kinetic Model. An autocatalytic kinetic model has been developed for assembly processes in which the array surface catalyzes the rate-determining formation of a critical "nucleus" (or "seed").

This autocatalytic model (see details in the Experimental Procedures) provides excellent fits for porphyrin assembly kinetic data and for the formation of amyloid from heated, acidic insulin solutions. Among our findings in this earlier work on the kinetics of insulin gelation is that certain metalloporphyrin derivatives are effective at inhibiting the rate of gel formation. At low concentrations of these inhibitors, the kinetic parameters remain relatively unchanged but the onset of the growth burst characteristic of gel formation can be delayed by a considerable time interval depending upon the porphyrin derivative selected and its concentration. We concluded that either the inhibition of the amyloid formation reaction occurs prior to the formation of the catalytic surfaces and/or the catalytic surfaces are modified or "poisoned", thereby rendering them incapable of catalysis.

In the present study, time-course kinetic and absorbance measurements have been augmented and correlated with AFM studies of the insulin structures formed along the kinetic pathway until final fibril and gel formation. The aim of this study is to more fully elucidate the mechanism of the inhibition by putative inhibitors of insulin fibrillation.

EXPERIMENTAL PROCEDURES

Reagents. Bovine insulin powder (Sigma-Aldrich) was stored in a desiccator at 0 °C and used without further purification. Insulin solutions were prepared daily, and concentrations were determined by absorbance at 278 nm (ϵ_{278} = 6040 M^{-1} cm^{-1}) (*20*). Standard reagents were

* To whom correspondence should be addressed. Telephone: 410-337-6288. Fax: 410-337-6408. E-mail: ssibley@goucher.edu.

‡ Goucher College.

§ Present address: Department of Forensic Sciences, George Washington University, Washington, D.C. 20052

|| Swarthmore College.

⊥ Present address: Department of Chemistry, University of California, Santa Barbara, CA 93106.

[1] Abbreviations: AFM, atomic force microscopy; TPPS, tetrakis(4-sulfonatophenyl)porphyrin; TAPP, tetrakis(4-*N*,*N*,*N*-trimethylanilinium)porphine; TMPyP, tetrakis(4-*N*-methylpyridyl)porphine.

10.1021/bi701682r CCC: $40.75
Published on Web 01/26/2008

obtained from Fisher. Nanopure water was used for all solutions. Water was filtered through a Nalgene 0.2 μm syringe filter prior to use.

Porphyrins, tetrakis(4-sulfonatophenyl)porphine (H_2TPPS) as well as metallated Pd^{II}TPPS, Cu^{II}TPPS, and Fe^{III}TPPS, were obtained from Frontier Scientific and used as received. Ni^{II}TPPS was synthesized by metal insertion into the free-base porphyrin (*21*). The cationic porphyrins tetrakis(4-*N*,*N*,*N*-trimethylanilinium)porphine (H_2TAPP) and Fe^{III}TAPP were purchased from Frontier Scientific.

Stock porphyrin solutions were prepared weekly. Concentrations of porphyrin solutions were determined using literature values for molar absorptivity. Porphyrins were studied in the range from 1×10^{-7} to $\sim 1 \times 10^{-5}$ M.

Instruments and Methods. Absorbance spectra were obtained with a Unicam UV4 spectrophotometer. Extinction measurements were made using Jasco V-530 UV/vis spectrophotometers with temperature control. Polymethylmethacrylate cuvettes were used for UV/vis and kinetic measurements.

Surface images were generated using a Quesant Instruments atomic force microscope run in WaveMode. Mixtures of fibrils and solutions were placed on freshly cleaved mica discs (Ted Pella, Inc.). The liquid phase was wicked away, and mica/fibril samples were allowed to air-dry prior to analysis.

Details of the standard protocol for kinetic measurements of insulin aggregation have been published previously (*22*). Briefly, a methylmethacrylate cuvette containing all reagents other than insulin was allowed to thermally equilibrate at the desired temperature (65 °C) in a heater block of a spectrophotometer. A small aliquot of insulin was added to the thermally equilibrated solution; the solution was mixed; and extinction measurements were initiated.

Kinetic Model. The model describes growth of a critical nucleus comprised of m aggregating solute units. The distinguishing feature of this model is a time-dependent rate constant that reflects catalysis by a growing surface (in this instance, the protein assembly)

$$k(t) = k_o + k_c(k_c t)^n \quad (1)$$

In eq 1, k_o and k_c are time-independent constants (both having units of s^{-1}) for the uncatalyzed and catalyzed aggregation, respectively. The time-dependent parameter n is related to the growth rate of the activating surface. The integrated rate law for this model ($m \neq 1$) is given by

$$[P]_t = [P]_\infty + ([P]_o - [P]_\infty)/\left(1 + (m-1)\left\{k_o t + (n+1)^{-1}(k_c t)^{n+1}\right\}\right)^{1/m-1} \quad (2)$$

where $[P]_\infty$ is the concentration of the monodispersed solute species at infinite time and $[P]_o$ is the initial concentration of the monodispersed entity. For the special case in which $m = 1$ (which corresponds to activation of the unassembled, initial solute species by the array surface as the rate-determining step), the equation takes on a more familiar form referred to as a "stretched exponential"

$$[P]_t = [P]_\infty + ([P]_o - [P]_\infty)\exp\left(-k_o t - (k_c t)^{n+1}/n+1\right) \quad (3)$$

(Note that for $n = 0$, eq 3 reverts to a simple exponential form). This form of the integrated rate law was introduced into the chemical literature by Avrami, for the analysis of polymer crystallization kinetics. Unlike the semiempirical Avrami approach, no requirement for integral values of n are imposed here.

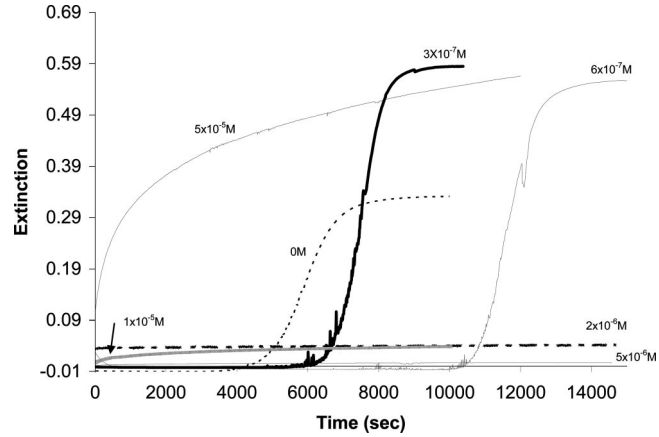

FIGURE 1: Kinetic profiles of insulin aggregation in the presence of varying concentrations of NiTPPS compared to an insulin standard.

Kinetic profiles were fitted through an application of the kinetic model described earlier with the use of Kaleidagraph software.

RESULTS

Kinetics. At pH 1.2 and 65 °C, all of the anionic metalloporphyrins studied are capable of inhibiting insulin fibrillation. For NiTPPS at low concentrations, e.g., 3×10^{-7} M, the inhibition is manifested as an extension of the lag time of the kinetic curve (type I behavior), with extinction monitored at 620 nm (Figure 1). The kinetic parameters for the fits with added metalloporphyrins are the same as for insulin run without added porphyrin when the incubation time is normalized (*16*). The porphyrin compounds PdTPPS and CuTPPS show similar inhibition ability at low concentrations, although the copper compound is the most effective at extending the lag time. Kinetic parameters of the reactions with several porphyrins are included in a previous paper (*16*). All of the above metalloporphyrins show a transition to a markedly different kinetic behavior at concentrations above $\sim 1 \times 10^{-6}$ M. For these higher concentration samples, aggregation begins immediately and the kinetic profile follows first-order (type II) behavior (see Figure 1, high concentrations, e.g., 5×10^{-5} M). For type II behavior, except at very high porphyrin concentration ranges, the final extinction value is generally considerably lower than that for the same metalloporphyrin exhibiting type I behavior.

As noted in an earlier study, FeTPPS is not as effective at inhibition as other TPPS metalloporphyrins; it causes less extension of the lag period at concentrations $\leq 10^{-6}$ M. It does show first-order kinetic behavior but only at considerably higher concentrations of added porphyrin ($\sim 1 \times 10^{-5}$ M). However, as was described in previous studies (*16*), the inhibition by FeTPPS persists even if the insulin sample is agitated, unlike the case for other derivatives.

In summary, for the anionic porphyrins studied, the efficiency of inhibition appears to be as follows:

$$CuTPPS^{4-} \sim NiTPPS^{4-} > PdTPPS^{4-} > FeTPPS^{3-} > H_4TPPS^{2-}$$

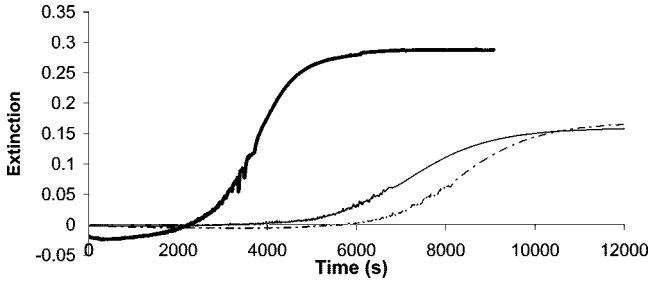

FIGURE 2: Kinetic profiles of insulin aggregation in the presence of varying concentrations of TAPP compared to an insulin standard. Dashed line, standard run; thin solid line, 3×10^{-7} M TAPP; thick solid line, 3×10^{-6} M TAPP.

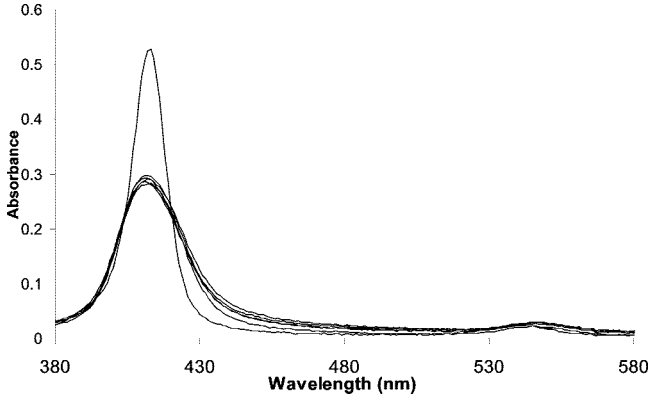

FIGURE 3: Absorbance data for samples at 1.7×10^{-6} M CuTPPS in 0.05 M HCl with increasing amounts of added insulin. The concentration ranges from 0 (top curve) to 1.02×10^{-4} M insulin.

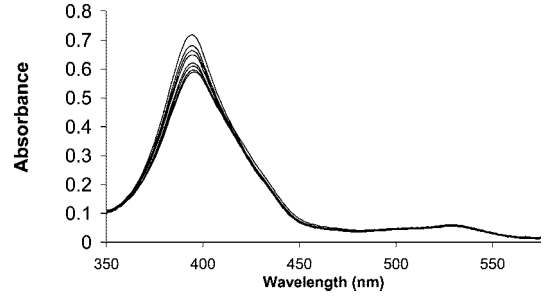

FIGURE 4: Absorbance data for samples at 4.7×10^{-6} M FeTPPS in 0.05 M HCl with increasing amounts of added insulin. The concentration ranges from 0 (top curve) to 9.4×10^{-5} M insulin.

In which the total charges of the derivatives are shown explicitly.

In contrast, the positively charged porphyrin H_4TAPP^{+6} and its metalloderivative $FeTAPP^{5+}$, similar to the cationic porphyrins previously tested belonging to the TMpyP family, do not inhibit insulin aggregation. In fact, H_4TAPP and FeTAPP appear to actually promote the aggregation process by decreasing the observed lag time (Figure 2).

Absorbance. The CuTPPS Soret band intensity (at approximately 410 nm) decreases markedly immediately upon the addition of insulin, indicative of binding to the native protein (Figure 3). The UV/vis absorbance spectrum for FeTPPS displays a Soret peak about 390 nm. The decrease in absorbance is much smaller in magnitude than that observed for the CuTPPS under similar conditions (Figure 4), and only a very minor shift in the absorbance maximum is observed. The FeTPPS absorbance change suggests that

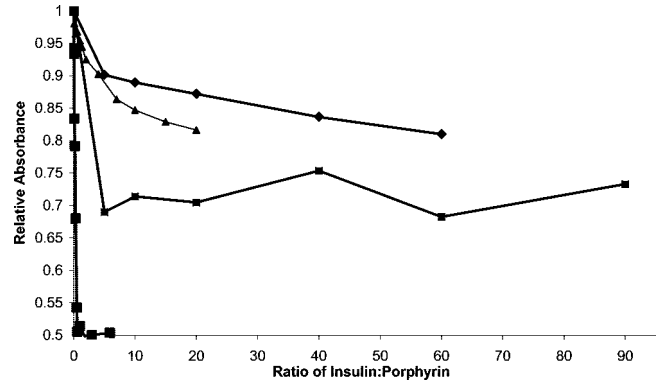

FIGURE 5: Absorbance changes as a function of the insulin/porphyrin ratio.

the binding does not involve axial coordination, because this would be expected to result in a much more significant bathochromic shift of the Soret peak (*23*). Axial ligation is not an option for the other derivatives. The absorbance maxima of the Q bands is typical of monomeric FeTPPS; peaks at longer wavelength would indicate dimeric porphyrin complexes (*24*). The unmetallated tetraphenylporphinesulfonate is protonated in acidic solution ($pK_a = 4.8$) forming the diacid (H_4TPPS^{2-}) that has been shown to bind proteins with an accompanying decrease in the Soret band intensity (*25*). UV/vis spectra obtained at pH 1.2 at the concentrations used in this study show that the porphyrin is indeed protonated, but a modest decrease in Soret band absorbance is observed upon the addition of insulin.

When the relative absorbance of the porphyrins is plotted as a function of the ratio of insulin/porphyrin, it is observed that CuTPPS appears to be completely bound at a relatively low ratio, indicative of tight binding (Figure 5). On the basis of these trends, the binding strength appears to mirror the inhibition efficiency observed in aggregation experiments.

AFM. Atomic force microscope scans were performed on samples from a standard insulin aggregation experiment (no metalloporphyrin added) at 65 °C (parts a and b of Figure 6). At early times during the lag period of the aggregation, the primary structures observed are small spherical particles (Figure 6a). These spherical particles are consistent with structures observed in high-resolution AFM studies early in the reaction process for insulin (*26*). At later times in the reaction, as the extinction begins to rise, fibrillar structures are observed. The number of the fibrils continues to increase as the reaction proceeds. In addition, fibrils appear to wind around each other, eventually forming rope-like structures (Figure 6b).

To probe the nature of the effect of porphyrin on aggregate structure, measurements were made of NiTPPS at low concentrations (3×10^{-7} M). A time-course kinetic measurement sampled at various points (Figure 7a) is shown in parts b−d of Figure 7. Initially (Figure 7b), only small spherical structures are observed. Although the reaction is inhibited, when fibrils finally appear, they are similar in structure to those formed during a standard insulin run in the absence of porphyrin (Figure 7d). However, new, apparently circular, ring-like structures were observed at intermediate times, prior to fibril formation and just prior to the rapid rise in extinction (Figure 7c). These structures have a diameter of approximately 100 nm. The size of bovine insulin at acidic conditions is approximately ~1 nm;

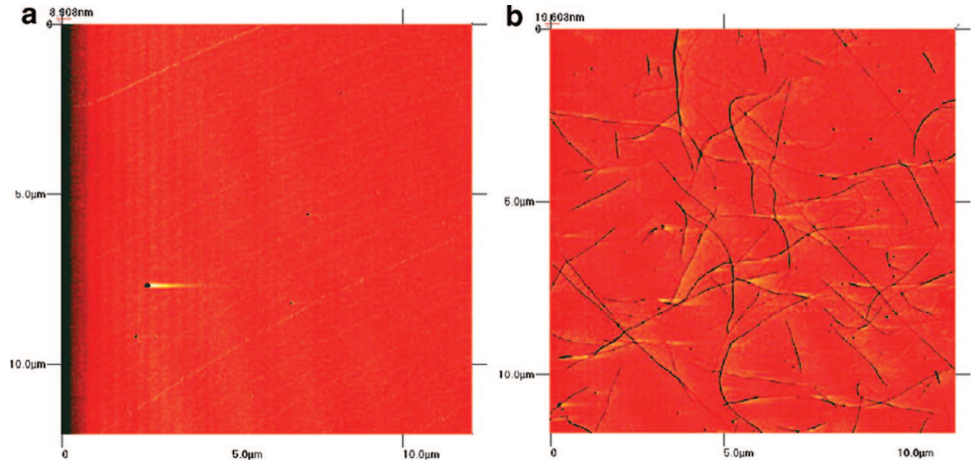

FIGURE 6: AFM images of a standard insulin sample (200 μM insulin and 0.05 M HCl) (a) after 2700 s and (b) after 6000 s.

therefore, the objects observed in the AFM slide are composed of ~100 insulin molecules. At high concentrations (10 μM) of NiTPPS (type II behavior), circular structures are again observed. As the reaction proceeds and extinction increases, the number of circular structures grows dramatically as well (parts a−d of Figure 8). As seen in Figure 8c, these circular structures aggregate together to form joined-ring structures. Under higher resolution, the ring-like structures are shown to be ring-like but appear to be composed of two semicircular units. No fibrillar structures are observed at any time.

AFM scans were also made for kinetic runs with added FeTPPS, the porphyrin that inhibits less effectively but whose inhibitory properties withstand agitation of the solution (*16*). Measurements at low concentration (3×10^{-7} M) eventually show fibril formation. However, in this case, the fibrils appear segmented (Figure 9). At higher resolution, some of the structures appear to be linear chains of the ring-like structures found in type II behavior for the other porphyrins. While it is possible that the segmenting is due to damage caused by the AMF scans, this is unlikely to be the case, because the segmenting is often not in the scan direction. At higher concentrations of FeTPPS where first-order kinetic behavior is observed, satisfactory images cannot be obtained, because of the mass of material.

Fibrils formed with added FeTAPP or TAPP appear similar to normal fibrils, although perhaps with slightly more curvature.

Spiking with Preformed Insulin Fibril. Spiking experiments were performed by spiking reactions with preformed insulin gels just prior to the rapid rise. This did not affect the kinetics of a standard insulin run, suggesting that prefibrillar species must have already been present in the solution. For an insulin kinetic run containing NiTPPS, however, spiking the reaction with preformed gel at 1550 s caused the lag time to shorten dramatically compared to an unspiked insulin/NiTPPS reaction, with the rise in extinction beginning almost immediately after the addition of preformed gel (Figure 10).

DISCUSSION

The current study attempts to correlate reaction profiles for the production of amyloid gels with the formation of structural entities in the reaction mixture. The results support the mechanism for gel formation proposed earlier, in which extended fibril surfaces serve as catalysts for the assembly process. In the absence of inhibitors, the AFM images show few fibrils during the so-called "incubation" or "quiescent" portion of the reaction. The growth burst typical of amyloid gel formation is concomitant with an increase in the number of these fibrils.

When metalloporphyrin inhibitors are added, various structures are observed. In some instances small, curved entities are formed involving tens of protein units. These structures can link for some porphyrin derivatives, but none lead to the growth burst seen in the absence of inhibitors. At low porphyrin concentrations, such small, abnormal structures are observed for extended periods, and it is theorized that only when the metalloporphyrins are depleted does a growth burst appear. Thus, protein aggregation is not "shut off" in the presence of these substances, but the aggregates formed are not capable of catalysis. When preformed fibril is spiked into the reaction mixture during a run, the fresh unpoisoned surfaces added overwhelm the ability of the porphyrins to continue the inhibition, resulting in an immediate growth burst.

Amyloid gel formation by insulin is known to be highly sensitive to solution conditions and the primary structure of the protein (*27*). Certain regions and sequences of amino acids, such as the histidine B10 site, are reported as being especially critical to the aggregation process. A common feature of all amyloid fibrils is a "steric zipper", in which sequences of side-chain residues interdigitate to form an interface free of solvent (*28*), which is critical to the aggregation and gives fibrils their robustness. For insulin, two such sequences are known to be crucial to the formation of amyloid-type fibrils (*29*), with one sequence on each of the A and B chains (*30*). The above-noted B10 histidine residue is just next to the leucine residue of one such fibril-forming sequence. While previous inhibition studies using so-called "stress molecules" (such as trehalose) have suggested that changes in solution surface tension and insulin hydration are responsible for the inhibition by these compounds, at the low concentrations used in this study, such an explanation cannot be the primary basis for porphyrin activity. Instead, our results point to interactions of the porphyrins with specific residues of the peptide chain that influence the hydrophobic interactions and zippering effects that drive fibril formation.

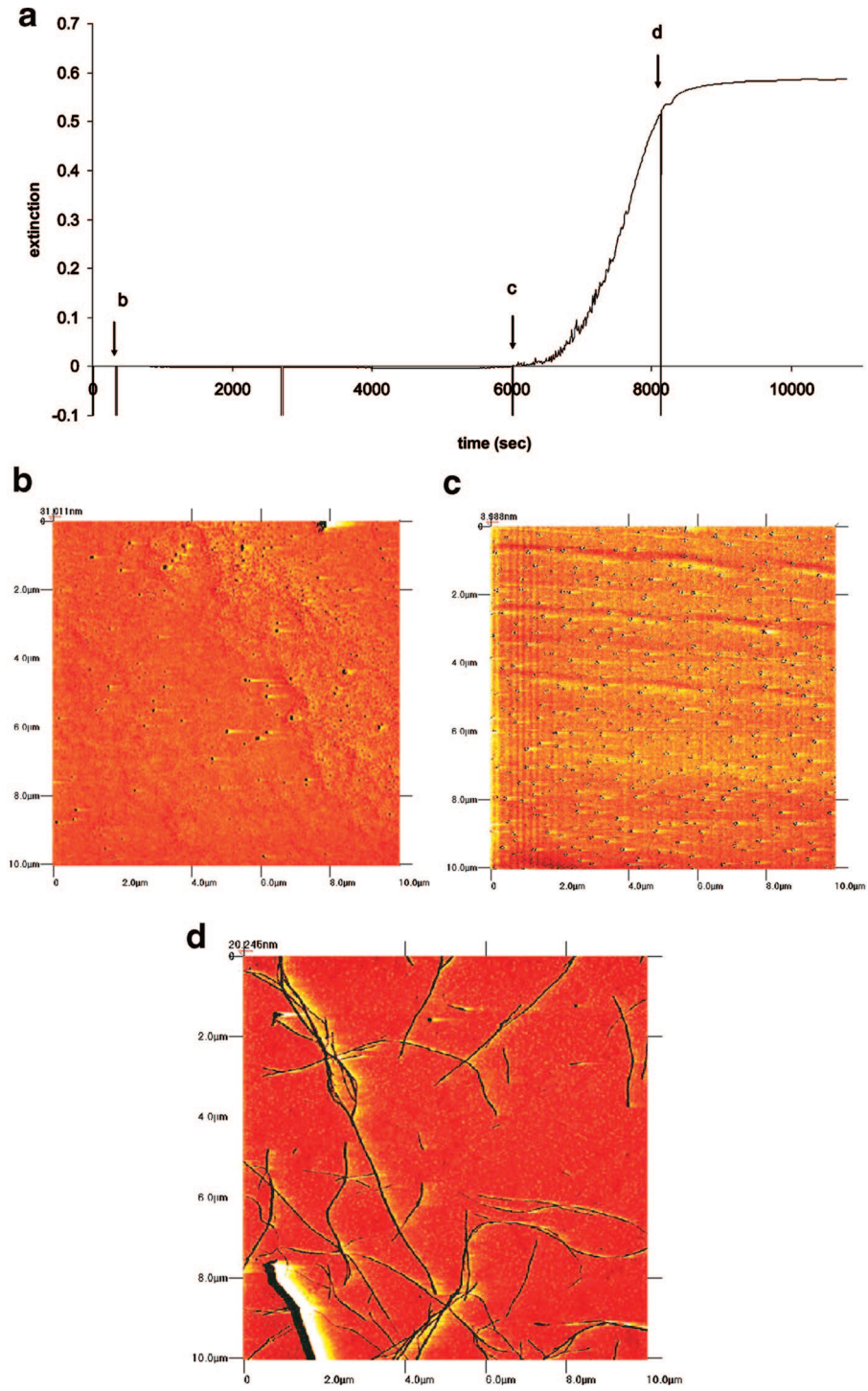

FIGURE 7: AFM study of 3×10^{-7} M NiTPPS, 200 μM insulin, and 0.05 M HCl. (a) Kinetic run data with sampling points noted for the following figures: AFM image (b) after 300 s, (c) after 6000 s, and (d) after 8100 s.

We have considered two classes of cationic porphyrins (TMpyP and TAPP) that differ markedly in their basicity, and neither has proven effective at inhibiting gel formation. It is worth noting that both positively and negatively charged porphyrin compounds have been shown to increase the survival time of mice when used prophylactically to treat scrapie (*31*). It is possible that the failure of the cationic porphyrins here may be related to the low pH conditions required to induce insulin amyloid gel formation. The positive charge on certain protonated amino acid residues may serve to repel cationic porphyrins from these sites. In contrast, anionic porphyrins are shown to demonstrate inhibition of insulin aggregation; the interaction likely involves attraction of the anionic porphyrins to the cationic insulin. Histidine is a likely candidate for porphyrin binding; it is protonated at low pH and, as mentioned earlier, is at a crucial location for gel formation.

However, such simple considerations of overall charge are not sufficient to account for the trends in porphyrin behavior. Differences in inhibition effectiveness of the various porphyrin derivatives correlate with the strength of binding of these molecules, as determined from absorption spectra. Issues of porphyrin self-aggregation tendency, as well as structure/charge buildup at the porphine core also appear to

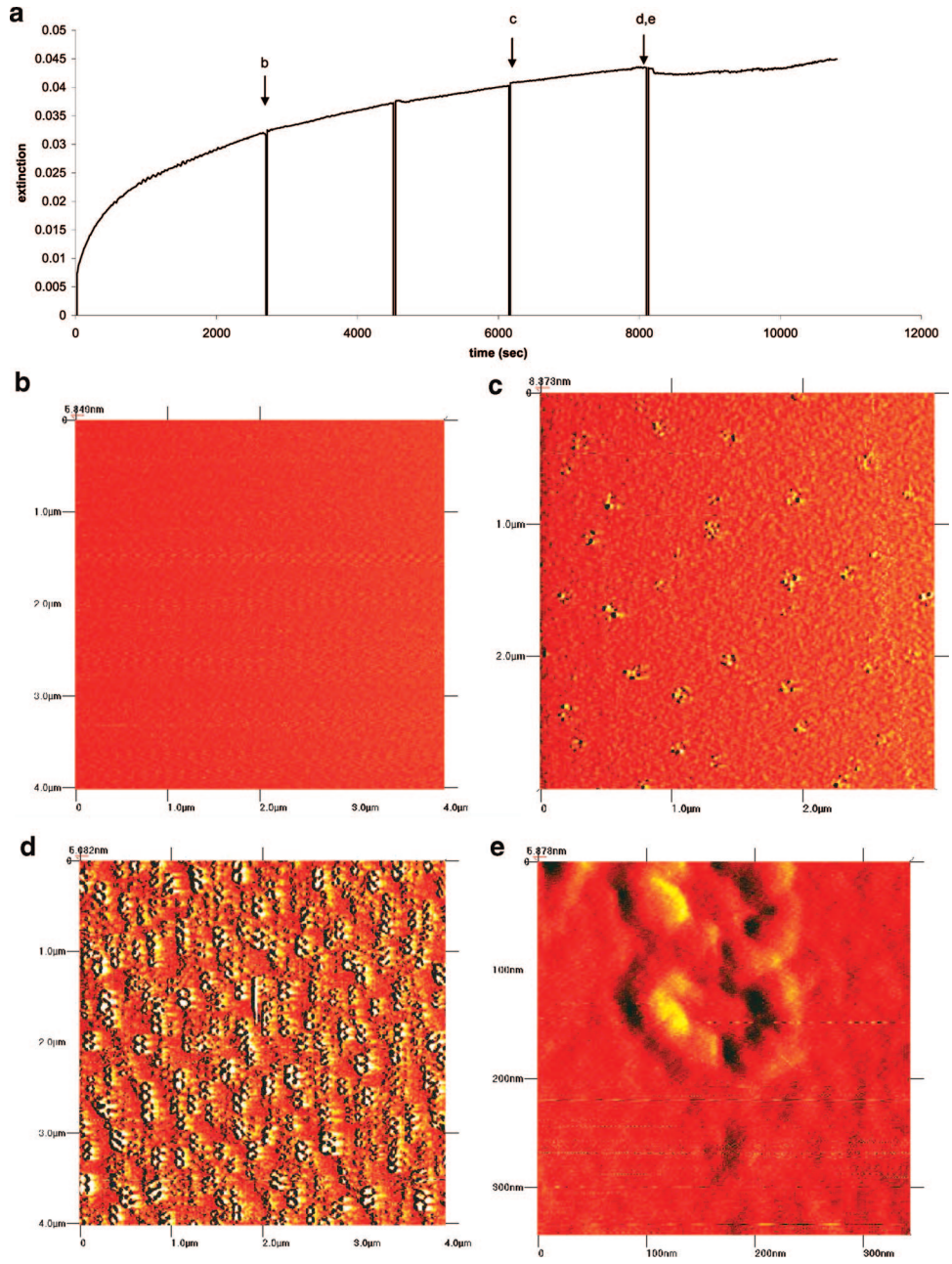

FIGURE 8: AFM study of 1×10^{-5} M NiTPPS, 200 μM insulin, and 0.05 M HCl. (a) Kinetic data with sampling points noted for the following figures: AFM image (b) after 2700 s and (c) after 6000 s, and (d) after 8100 s. (e) Closer view of the segmented regions seen in d.

play a role. The nonmetallo porphyrin, a dianion but with a buildup of 2+ charge at the core and a "buckled" structure is the least effective at inhibiting gel formation. The weaker inhibition by FeTPPS than other metal derivatives tested suggests that the more positive core (Fe^{3+} versus the other divalent metals) affects the electron density distribution in the ring system and thereby affects the interaction with the insulin-binding site.

The addition of porphyrins at low concentrations (type I behavior) extends the lag period for aggregation but generally results eventually in fibrils that appear similar to those from insulin alone. The results of the present AFM studies (Figure 7) are consistent with conclusions drawn from the kinetic model proposed for gel formation; the process is catalyzed by the surfaces of the assemblies formed en route to the product. Deformation of these surfaces leads to significantly extended quiescent periods prior to the growth bursts associated with gel formation; i.e., the deformed surfaces lose the ability to catalyze the process. The dramatic changes in the aggregate structure are more easily seen at somewhat higher concentrations of metalloporphyrin. Similar to the results observed by adding pure A- or B-chain insulin to a normal insulin mixture (*32*), the addition of porphyrins at higher concentrations causes morphological changes as a result of changes in the packing of insulin molecules as well as changes to the kinetic profile. In Figure 8, for example, very little gel is formed for 10 μM NiTPPS even after 12 000 s. The influence of porphyrin binding clearly causes major changes in the normal insulin linkages that occur during fibril growth. Also in Figure 9, for FeTPPS, the circular structures observed at early times in the aggregation may be incorpo-

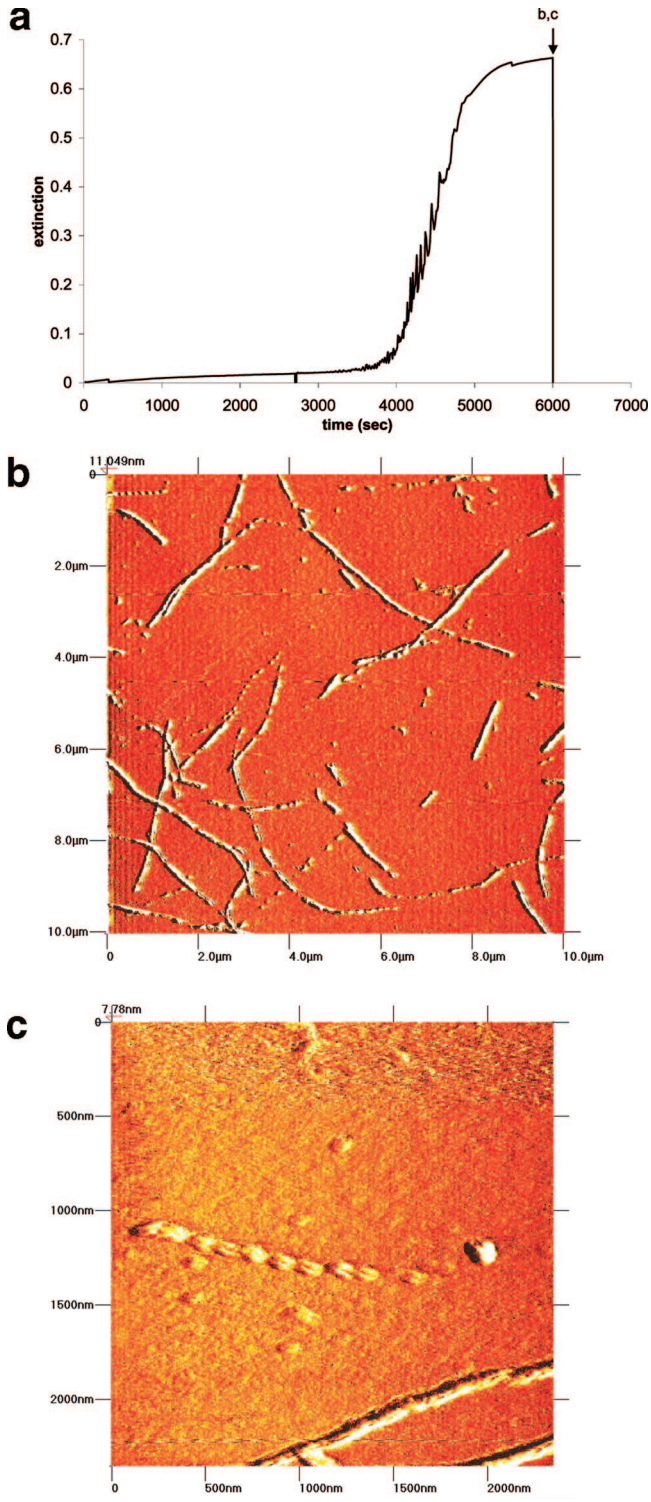

FIGURE 9: AFM study of 3×10^{-7} M FeTPPS, 200 μM insulin, and 0.05 M HCl. (a) Kinetic data. (b) AFM sample at 6000 s. (c) Closer view of b.

rated into fibrils but also may self-aggregate to form large, amorphous structures.

As described earlier, at higher porphyrin concentrations, several derivatives demonstrate an alternative, first-order kinetic pathway that, in general, is far less efficient at producing gels. We believe that this new pathway may be based on the ability of these derivatives to form dimers or other small aggregates that provide a rather inefficient catalytic surface for some gel formation. All of Cu^{II}-, NI^{II}-,

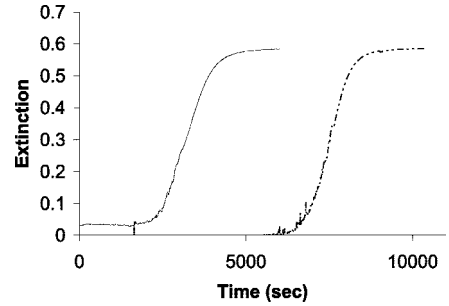

FIGURE 10: Kinetic profiles of 3×10^{-7} M NiTPPS, one without spiking and one that was spiked after 1550 s.

and Pd^{II}TPPS are known to dimerize even at low concentrations in aqueous solution (*33*). While the iron porphyrins have often been associated with μ-oxo dimers, this form is not likely under the acidic conditions used here. However, Fe^{III} porphyrins have been shown to form $\pi-\pi$ dimers as well, albeit with less tendency that the metal(II) derivatives studied here. The lower tendency of dimerization of the iron porphyrin is also consistent with the higher concentration required for the onset of first-order aggregation behavior.

These observations concerning the insulin amyloid assembly mechanism suggest an alternative strategy for drug design for preventing or at least decelerating the onset of Alzheimer's disease. Small molecules capable of preferential binding to amyloid fibrils and also capable of modifying the tertiary/quaternary structure of these peptide assemblies could prove useful in the prevention and treatment of the disease. Derivatives that have little tendency to self-aggregate would be particularly attractive to avoid alternative pathways to gel formation and may be of interest for inhibition studies on many amyloid systems.

ACKNOWLEDGMENT

The authors thank Goucher College for summer support.

REFERENCES

1. Harper, J. D., Jr. (1997) Models of amyloid seeding in Alzheimer's deisease and scrapie: Mechanistic truths and physiological consequences of the time-dependent solubility of amyloid proteins. *Annu. Rev. Biochem. 66*, 385–407.
2. Kosik, K. S. (1994) The Alzheimer's disease sphinx: A riddle with plaques and tangles. *J. Cell Biol. 127*, 1501–1504.
3. Cookson, M. (2005) The biochemistry of Parkinson's disease. *Annu. Rev. Biochem. 74*, 29–52.
4. Goers, J., Permyakov, S. E., Permyakov, E. A., Uversky, V. N., and Fink, A. L. (2002) Conformationoal prerequisites for α-lactalbumin fibrillation. *Biochemistry 41*, 12546–12551.
5. Nelson, R., Sawaya, M. R., Balbirnie, M., Madsen, A. O., Riekel, C., Grothe, R., and Eisenberg, D. (2005) Structure of the cross-β spine of amyloid-like fibrils. *Nature 435*, 773–778.
6. Padrick, S. B., and Miranker, A. D. (2002) Islet mayloid: Phase partitioning and secondary nucleation are central to the mechanism of fibrillogenesis. *Biochemistry 41*, 4694–4703.
7. Taboada, P., Barbosa, S., Castro, E., and Mosquera, V. (2006) Amyloid fibril formation and other aggregate species formed by human serum albumin association. *J. Phys. Chem. B 110*, 20733–20736.
8. Thorn, D. C., Meehan, S., Sunde, M., Rekas, A., Gras, S. L., MacPhee, C. E., Dobson, C. M., Wilson, M. R., and Carver, J. A. (2005) Amyloid fibril formation by bovine milk κ-casein and its inhibition by the molecular chaperones α_S- and β-casein. *Biochemistry 44*, 17027–17036.
9. Nielsen, L., Frokjaer, S., Brange, J., Uversky, V. N., and Fink, A. L. (2001) Probing the mechanism of insulin fibril formation with insulin mutants. *Biochemistry 40* (28), 8397–8409.

10. Millican, R. L., and Brems, D. N. (1994) Equilibrium intermediates in the denaturation of human insulin and two monomeric insulin analogs. *Biochemistry 33*, 1116–1124.
11. Krebs, M. R. H., Bromley, E. H. C., Rogers, S. S., and Donald, A. M. (2005) The mechanism of amyloid spherulite formation by bovine insulin. *Biophys. J. 88*, 2013–2021.
12. Murali, J., and Jayakumar, R. (2005) Spectroscopic studies on native and protofibrillar insulin. *J. Struct. Biol. 150*, 180–189.
13. Hua, Q., and Weiss, M. A. (2004) Mechanism of insulin fibrillation: The structure of insulin under amyloidogenic conditions resembles a protein-folding intermediate. *J. Biol. Chem. 279*, 21449–21460.
14. Manno, M., Craparo, E. F., Martorana, V., Bulone, D., and San Biagio, P. L. (2006) Kinetics of insulin aggregation: Disentanglement of amyloid fibrillation from large size cluster formation. *Biophys. J. 90*, 4585–4591.
15. Librizzi, F., and Rischel, C. (2005) The kinetic behavior of insulin fibrillation is determined by heterogeneous nucleation pathways. *Protein Sci. 14*, 3129–3134.
16. Pasternack, R. F., Gibbs, E. J., Sibley, S., Woodard, L., Hutchinson, P., Genereux, J., and Kristian, K. (2006) Formation kinetics of insulin-based amyloid gels and the effect of added metalloporphyrins. *Biophys. J. 90*, 1033–1042.
17. Khurana, Ionescu-Zanetti, C., Pope, M., Li, J., Nielson, L., Ramirez-Alvarado, M., Regan, L., Fink, A. L., and Carter, S. A. (2003) A general model for amyloid assembly based on morphological studies using atomic force microscopy. *Biophys. J. 85*, 1135–1144.
18. Jansen, R., Dzwolak, W., and Winter, R. (2005) Amyloidogenic self-assembly of insulin aggregates probed by high resolution atomic force microscopy. *Biophys. J. 88*, 1344–1353.
19. Guo, S., and Akhremitchev, B. B. (2006) Packing density and structural homogeneity of insulin amyloid fibrils measured by AFM nanoindentation. *Biomacromolecules 7*, 1630–1636.
20. Frank, B. H., Veros, A. J., and Pekar, A. H. (1972) Physical studies on proinsulin. Comparison of the titration behavior of the tyrosine residues in insulin and proinsulin. *Biochemistry 11*, 4926–4931.
21. Pasternack, R. F., Francesconi, L., Raff, D., and Spiro, E. (1973) Aggregation of nickel(II), copper(II), and zinc(II) derivatives of water-soluble porphyrins. *Inorg. Chem. 12*, 2606–2611.
22. Pasternack, R. F., Gibbs, E. J., Collings, P. J., dePaula, J. C., Turzo, L. C., and Terracina, A. (1998) A nonconventional approach to supramolecular formation dynamics. The kinetics of assembly of DNA-bound porphyrins. *J. Am. Chem. Soc. 120*, 5873–5878.
23. Gibbs, E. G., Skowronek, W. R., Morgan, W. T., Muller-Eberhard, U., and Pasternack, R. F. (1980) Reactions of water-soluble metalloporphyrins with the serum protein, hemopexin. *J. Am. Chem. Soc. 102*, 3939–3944.
24. Yushmanov, J., Imasato, H., Tominaga, T. T., and Tabak, M. (1996) ^{1}H NMR and electronic absorption spectroscopy of paramagnetic water-soluble *Meso*-tetraarylsubstituted cationic and anionic metalloporphyrins. *J. Inorg. Biochem. 61*, 233–250.
25. Andrade, S., and Costa, S. M. (2002) Spectroscopic studies on the interaction of a water soluble porphyrin and two drug carrier proteins. *Biophys. J. 82*, 1607–1619.
26. Jansen, R., Dzwolak, W., and Winter, R. (2005) Amyloidogenic self-assembly of insulin aggregates probed by high resolution atomic force microscopy. *Biophys. J. 88* (2), 1344–1353.
27. Nielsen, L., Frokjaer, S., Brange, J., Uversky, V. N., and Fink, A. L. (2001) Probing the mechanism of insulin fibril formation with insulin mutants. *Biochemistry 40* (28), 8397–8409.
28. Nelson, R., Sawaya, M. R., Balbirnie, M., Madsen, A. O., Riekel, C., Grothe, R., and Eisenberg, D. (2005) Structure of the cross-β spine ofamyloid-like fibrils. *Nature 435*, 773–778.
29. Ivanova, M. I., Thompson, M. J., and Eisenberg, D. (2006) A systematic screen of β_2-microglobulin and insulinfor amyloid-like segments. *Proc. Natl. Acad. Sci. U.S.A. 103*, 4079–4082.
30. Hong, D.-P., Ahmad, A., and Fink, A. L. (2006) Fibrillation of human insulin A and B chains. *Biochemistry 45*, 9342–9353.
31. Kocisko, D. A., Caughey, W. S., Race, R. E., Roper, G., Caughey, B., and Morrey, J. D. (2006) A porphyrin increases survival time of mice after intracerebral prion infection. *Antimicrob. Agents Chemother. 50*, 759–761.
32. Devlin, G., Knowles, T. P., Squires, A., McCammon, M. G., Gras, S. L., Nilsson, M. R., Robinson, C. V., Dobson, C. M., and MacPhee, C. E. (2006) The component polypeptide chains of bovine insulin nucleate or inhibit aggregation of the parent protein in a conformation-dependent manner. *J. Mol. Biol. 360*, 497–509.
33. Corsini, A., and Hermann, O. (1986) Aggregation of *meso*-tetra-(*p*-sulphonatophenyl)porphine and its Cu(II) and Zn(II) complexes in aqueous solution. *Talanta 33*, 335–339.

BI701682R